JACS Au
AN OPEN ACCESS JOURNAL OF THE AMERICAN CHEMICAL SOCIETY

pubs.acs.org/jacsau
Article

Tertiary-Amine-Functional Poly(arylene ether)s for Acid-Gas Separations

Pablo A. Dean,[§] Yifan Wu,[§] Sheng Guo, Timothy M. Swager,* and Zachary P. Smith*

Cite This: JACS Au 2024, 4, 3848−3856
Read Online

ACCESS | Metrics & More | Article Recommendations | Supporting Information

ABSTRACT: Competitive sorption enables the emergent phenomenon of enhanced CO_2-based selectivities for gas separation membranes when using microporous polymers with primary amines. However, strong secondary forces in these polymers through hydrogen bonding results in low solvent solubility, precluding standard solution processing approaches to form these polymers into membrane films. Herein, we circumvent these manufacturing constraints while maintaining competitive-sorption enhancements by synthesizing eight representative microporous poly(arylene ether)s (PAEs) with tertiary amines. High-pressure H_2S, CO_2, and CH_4 sorption isotherms were collected for these samples to demonstrate enhanced affinity for acid gases relative to the unfunctional control polymer. Although competitive sorption was observed for all samples, improvements were less pronounced than for primary-amine-functional analogs. For H_2S-based separations, the benefits of competitive sorption offset decreases in selectivity due to plasticization. This detailed study helps to elucidate the role of tertiary amines for acid gas separations in solution-processable microporous PAEs.

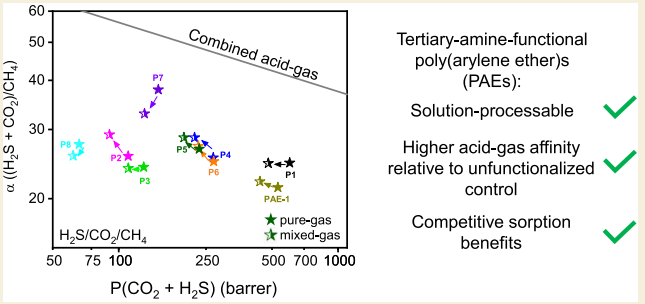

KEYWORDS: *polymer membrane, amine, carbon dioxide, hydrogen sulfide, gas separation*

Membranes offer an attractive alternative to legacy separation processes due to their energy-efficiency and ease of operation. In fact, membranes consume up to 90% less energy than distillation, which, if implemented broadly within the industrial chemicals industry, could translate to an estimated annual savings of 100 million tonnes of carbon dioxide (CO_2) emissions and $4 billion in energy cost savings.[1]

The application of membranes for direct CO_2-based separations is of particular interest for a sustainable future.[2−4] Membrane-based CO_2 separations are deployed in natural gas purification today, but the market share in this application is estimated at only about 10% when compared to more prevalent unit operations like amine absorption.[5,6] CO_2-based separations are urgently needed in other areas as well, most notably carbon capture, but technology adaption has been stubbornly slow.[7−9] On the contrary, a growing topic to meet energy needs and net-zero carbon goals is purifying biogas to make renewable natural gas (RNG). Unlike traditional natural gas, RNG offers a carbon-neutral source of fuel when purified from various sources like livestock waste and landfills.[10] Two common impurities in RNG that must be removed are CO_2 and hydrogen sulfide (H_2S). These acid gases are highly corrosive to pipelines and lower the heating value of the fuel. Conventionally, these gases are extracted via absorption into basic amine solutions, following techniques previously used in natural gas purification,[11,12] but amines are toxic and volatilize, so polymer-membrane based alternatives are appealing to avoid these issues while also adding the benefit of continuous operation and small physical footprint.[13] Polymer membranes have a well-known "upper-bound" trade-off limit in permeability (throughput) and selectivity (separation efficiency), which limits their use,[14] but recent advances in polymer chemistry through the discovery of polymers of intrinsic porosity (PIMs) and related "microporous" materials have pushed the limits of separation performance, offering a potential materials solution to CO_2-based separations.[15−20]

Membranes are normally evaluated using pure-gas measurements. However, these tests are often poor predictors of performance under realistic conditions,[1,21] where highly interacting gases like H_2S can severely plasticize the membrane and compromise its size-sieving ability.[22,23] Conversely, the effects of competitive sorption can be leveraged in mixtures, whereby more polarizable gases (CO_2, H_2S) can exclude supercritical ones (CH_4, N_2), thus enhancing selectivity relative to pure-gas calculations.[24,25] For example, recent work by our group has shown that primary-amine-functionalized PIM-1 (PIM-NH_2) and poly(arylene ether) (PAE-NH_2)

Received: June 7, 2024
Revised: July 17, 2024
Accepted: July 17, 2024
Published: October 2, 2024

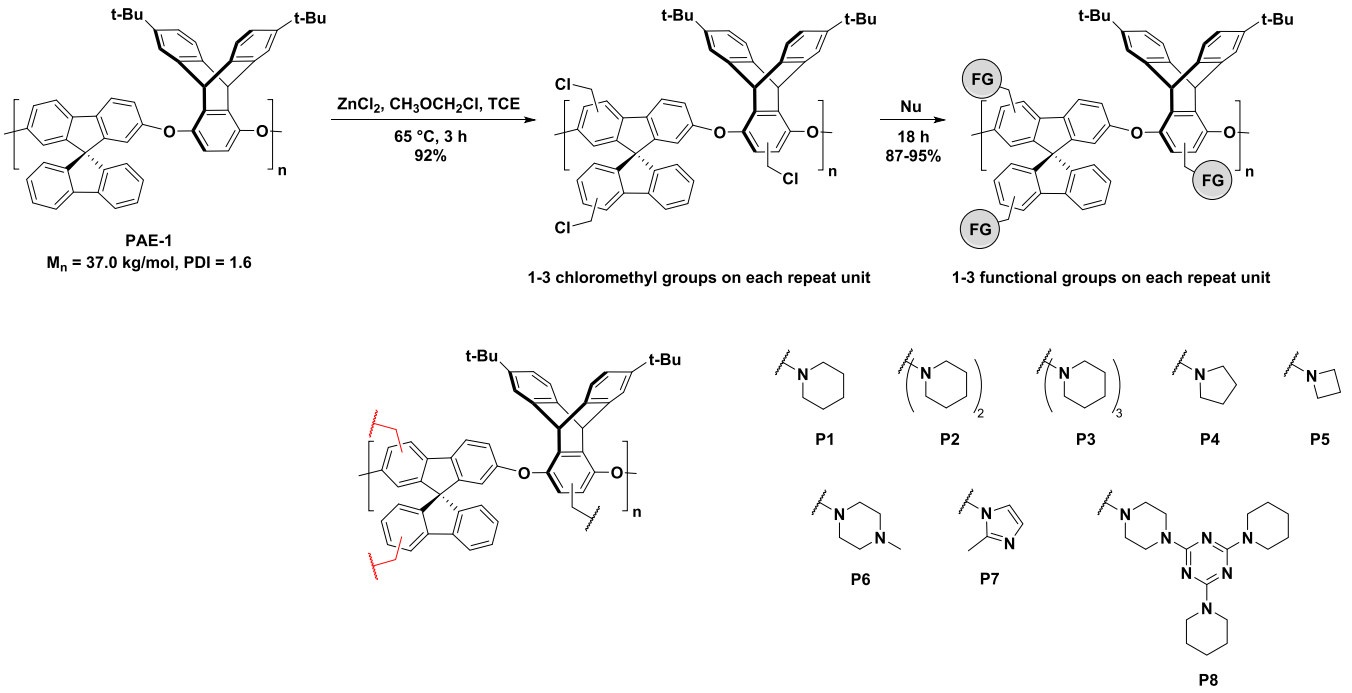

Figure 1. Synthetic scheme of amine-functionalized PAEs as membrane materials. The sites of functionalization are not precisely known and the drawing is intended to be representative. The bonds labeled in red represent sites where the additional side groups in the case of **P2** and **P3** are believed to attach. The detailed synthesis and characterization of each polymer can be found in the Supporting Information, and a table with the precise number of functional groups for each polymer is presented in Table S1.

exhibit more than a 2-fold increase in CO_2/CH_4 selectivity when tested with gas mixtures compared to sequential pure-gas experiments.[26,27] This increase was attributed to the enhanced gas−polymer affinity afforded by the amine functional group, which significantly reduced methane sorption.

Although the PIM- and PAE-based primary-amine-functional membranes show higher affinity for acid gases relative to their nitrile-functional counterparts, they are not solution-processable in common organic solvents, thereby limiting their industrial scalability. Additionally, primary amines are prone to oxidative degradation through a large number of mechanistic pathways.[28] Therefore, we hypothesized that installing pendant tertiary amines, instead of primary amines, would improve polymer solubility and stability while retaining strong interactions with CO_2 and H_2S, resulting in competition-enhanced separation performance. To test this hypothesis, we report the synthesis and transport properties of 8 novel tertiary-amine-functional polymers derived from our previously developed PAE backbone.[29]

The tertiary-amine-functional PAEs were synthesized via Pd-catalyzed C−O polycondensation, and subsequent postpolymerization modifications are summarized in Figure 1. Chloromethylation of the polymer backbone was followed by displacement of the chloride by amine-based nucleophiles to introduce a variety of functional groups, thereby forming a series of solution-processable microporous organic polymers. These polymers (**PAE-1-P1** through **PAE-1-P8**), which are synthesized from unfunctionalized **PAE-1**, are shown in Figure 1.

Amine functional groups were chosen based on their basicity and predicted affinity for acidic gases. Amine-based PAEs could be synthesized directly from monomers that contain amine groups. However, functional monomers often require multistep synthesis procedures with cumbersome purification steps. Postpolymerization modification eliminates these drawbacks, and PAEs benefit from their compatibility with electrophilic functionalization reactions. These functionalized polymers retain their solution-processability and form microporous-polymer films with chemical affinity for H_2S and CO_2.

In designing these new polymers, we considered two structural variables that were anticipated to correlate with gas permeability and selectivity: BET surface area and the nitrogen-to-carbon (N/C) ratio for amine side groups. Previously, Tröger's base-containing polyimides,[30] thermally rearranged (TR) polymers,[31] and tetraphenylethylene-based membrane materials[32] have shown markedly positive correlations between measured surface areas and CO_2 permeabilities. Additionally, Mizrahi Rodriguez et al. quantified that the aforementioned amine-functional PIM-NH_2 can increase sorption selectivity by more than a factor of 2 relative to unfunctionalized PIM-1.[27] The BET surface area and N/C ratio per monomer can be varied through the degree of functionalization, the ring size of the cyclic amines, and the fractional weight of nitrogen in each functional group. High degrees of functionalization are achieved by installing 2−3 chloromethyl groups onto each repeat unit during the first step of synthesis. By varying the ring size and hybridization of cyclic amines, we can tune the basicity of these amine groups, which can be impacted by the presence of neighboring electron-donating groups and additional resonance structures. The basicity of the functional groups with different ring sizes and structures is summarized in Table 1 using pK_a values of small molecule analogs, alongside Brunauer−Emmett−Teller (BET) surface areas and fractional free volume (FFV) values, which will be discussed in detail in the subsequent sections. Moreover, sorption experiments were used to analyze the effect of the amine groups on gas−polymer affinity relative to the unfunctionalized **PAE-1**. To study the effect of nitrogen

https://doi.org/10.1021/jacsau.4c00489
JACS Au 2024, 4, 3848−3856

Table 1. BET Surface Areas and FFV Values of Amine-Functional Polymers P1−P8, along with pK_a Values of the Small Molecule Amine Analogs of Each Polymer

	BET surface area (m^2 g^{-1})	FFV	pK_a
PAE-1	668[a]	22	n/a
P1	462	12	11.2
P2	74.6	10	11.2
P3	34.6	9	11.2
P4	25.3	8	11.3
P5	139	17	11.3
P6	215	22	9.1
P7	116	16	7.9
P8	7.0	13	5.1

[a]**PAE-1** surface area previously reported.[33]

density, nitrogen-rich functional groups such as methylpiperazine, methylimidazole, and melamine were incorporated onto the polymer backbone, providing N/C ratios as high as 0.6 per monomer for amine side groups.

BET surface areas of the amine-functionalized polymers were calculated according to commonly used fitting criteria[34] and are presented in Table 1, with the corresponding isotherms shown in Figure S2. Relative to the unfunctionalized control, functionalization results in a decrease in BET surface area for all samples. These features likely relate to stronger interchain interactions from the addition of polar heteroatoms and from the size of the appended moieties. Specifically, the hydrogen on the unfunctionalized control has a van der Waals volume of 3.35 cm^3 mol^{-1}, while the moieties on the functionalized polymers range from 45.0 cm^3 mol^{-1} for **P5** to 189 cm^3 mol^{-1} for **P8**, as calculated using the Monte Carlo simulation procedure outlined in the updated group contribution method by Wu et al.[35] A list of van der Waals volumes for all amine side groups can be found in Table S2, and corresponding densities and fractional free volume (FFV) values are shown in Table S3. Thus, functionalization of the chloromethylated polymers with large cyclic amines such as piperidine can occupy additional free volume and decrease the intrinsic porosity. Nevertheless, all polymers retained measurable surface areas, which to the best of our knowledge, is not reported for any poly(ether)s without free-volume-generating structural units. We also measured the *d*-spacing of each polymer by wide-angle X-ray scattering (WAXS), revealing similar characteristic patterns but a few salient differences in polymer packing, which will be discussed later (Figure S3).

Interestingly, functional group size had a very weak negative correlation with BET surface area (R^2 = 0.250), as can be observed in Figure S4a. In fact, a wide range of BET surface areas were measured for polymers with the smallest tertiary amine moieties. For example, the piperidinyl moiety in **P1** has a molar volume of 61.9 cm^3 mol^{-1} and a BET surface area of 462 m^2 g^{-1}, while the pyrrolidinyl moiety in **P4** has a molar volume of 58.4 cm^3 mol^{-1} and a BET surface area of only 25.3 m^2 g^{-1}. These findings demonstrate the difficulty of using the size of a functional moiety to predict the nascent packing structure of a glassy polymer, even for polymers with identical backbones. However, for a higher degree of functionalization with identical chemical moieties, a trend can be gleaned by comparing **P2** and **P3**, whereby BET surface area does decrease, albeit slightly. We further note that the validity of BET as a technique for quantifying accessible surface area in glassy polymers has been a matter of debate,[36,37] so our results indicate the need to avoid overinterpretation of BET surface areas when identifying good microporous polymers for membrane applications. Similar to BET surface area, functional group size has an even weaker negative correlation with FFV (R^2 = 0.151), as can be observed in Figure S4b (with corresponding discussion). A parity semilog plot between FFV and pure-gas CO_2 permeability (Figure S5) is also provided, showing another weak correlation (R^2 = 0.154) between the two values. Therefore, direct analysis of permeability is required to map out how trends in permeability correlate with these tertiary-amine-functional polymers.

Thermogravimetric analysis (TGA) was performed to evaluate the thermal degradation temperatures (T_d) of the polymers. Results, shown in Figure S6 and Table S4, indicate excellent thermal stability, with degradation temperatures higher than 300 °C for all samples. No glass transition temperatures (T_g) were observed for any of the polymers from differential scanning calorimetry (DSC) analysis, suggesting that the ultraglassy nature of these structures precludes long-range cooperative chain motion before the onset of high-temperature degradation. Although rare for conventional polymers and many rigid engineering thermoplastics, the lack of an observable T_g below the degradation temperature is

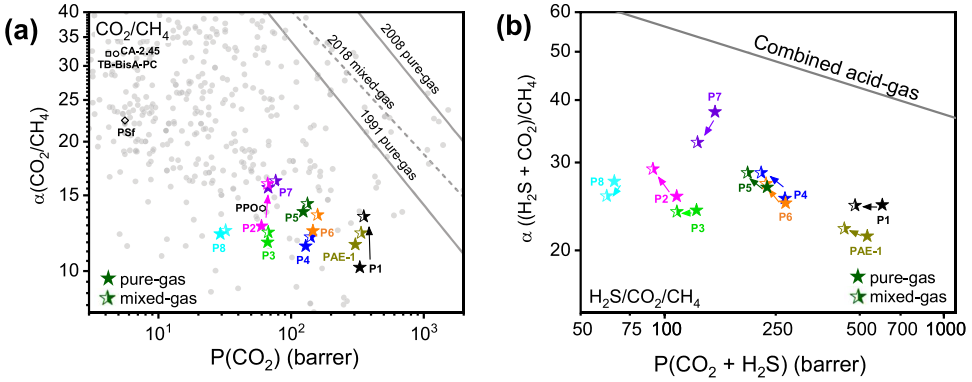

Figure 2. Separation performance in mixed-gas (half-filled stars) and pure-gas (filled stars) conditions for (a) binary (50:50 CO_2/CH_4 at 2.2 bar) and (b) ternary (20:20:60 $H_2S/CO_2/CH_4$ at 8 bar). Relevant upper-bound trendlines and pure-gas results from prior literature studies (gray circles) are shown for comparison.[14,43−46] The pure-gas data point for **P8** in a binary mixture was calculated using CH_4 permeability at f_{CH_4} = 4.7 bar instead of 1.1 bar due to the flux detection limit in the permeation system. PSf is polysulfone, TB-BisA-PC is tetrabromo bisphenol A polycarbonate, and CA-2.45 is cellulose acetate with 2.45% degree of acetylation. Arrows connect identical samples for pure- and mixed-gas tests.

https://doi.org/10.1021/jacsau.4c00489
JACS Au 2024, 4, 3848−3856

common for microporous polymers, unless measuring the T_g through specialized ultrafast scanning calorimetry techniques.[38] In fact, various types of PIMs, including PIM-1,[18,39] Tröger's base- and triptycene-based polymers,[16,40] thermally rearranged polyimides,[41] ROMP materials,[42] and CANAL polymers,[20] all lack an observable T_g below T_d when using standard DSC techniques. Therefore, the polymer family presented here should be categorized within this small but intriguing structural subclass of polymers that are of significant interest to the membrane field. Of similar importance, their high thermal stability suggests that functional PAEs may be stable in a diverse array of processing and reactivation conditions anticipated for industrial applications.

The utility of the amine-functionalized PAEs for biogas purification was evaluated through binary (CO_2/CH_4) and ternary ($H_2S/CO_2/CH_4$) pure- and mixed-gas permeation experiments. The results of these tests are plotted against the corresponding upper-bound trendlines[14,43−46] in Figure 2. Most notably, all samples exhibit slight increases in permselectivity in the mixed-gas binary tests relative to the pure-gas tests, illustrating potential competition enhancements, although these improvements are far less significant than for primary-amine-functional PIMs and PAEs. For example, **P1** had a 31% improvement in CO_2/CH_4 selectivity when tested with a mixture compared to the pure-gas calculation. Similar findings are reported for nonaminated microporous polymers such as PAE-5,[33] PIM-1,[27,47] and PAE-CN.[47] However, primary amines, such as PIM-NH_2, exhibit an 11-fold increase in selectivity for a similar comparison.[47] The unfunctionalized control sample, **PAE-1**, was also tested for reference. **PAE-1** only showed a 6% increase in CO_2/CH_4 selectivity. Note also that the corresponding pure-gas data point in the binary CO_2/CH_4 mixture for **P8** was evaluated at a higher pressure than that of the other samples because CH_4 flux was below the system detection limit at f_{CH_4} = 1.1 bar. The pure-gas data point shown for **P8** in Figure 2a was calculated using CH_4 permeability at f_{CH_4} = 4.7 bar, which is the same value used for calculating the corresponding pure-gas data point in the combined-acid-gas upper-bound plot.

Figure 2a indicates that none of the PAEs that exhibit observable selectivity boosts (**P1** and **P2**) lose significant permeability for CO_2 in the presence of CH_4 demonstrating the theoretically expected result that CH_4 is selectively excluded from the polymer while the co-permeation of CO_2 is relatively unaffected. Conversely, in the $H_2S/CO_2/CH_4$ mixture, the presence of two acidic gases competing with one another reduces membrane permeability for each gas, as illustrated by the leftward trajectory on the upper-bound plot in Figure 2b. This reduction in CO_2 and H_2S permeability is not accompanied by a boost in combined-acid-gas selectivity. Therefore, CO_2, H_2S, and CH_4 all co-permeate less readily through the membrane film compared to when they permeate independently, and the CH_4 permeability does not decrease sufficiently in the ternary mixture to further boost the overall permselectivity. As will be discussed, this lack of selectivity enhancement is likely attributed to a decrease in diffusion selectivity brought on by H_2S-induced plasticization.

The limited pure- to mixed-gas selectivity improvement and the aforementioned plasticization effect of H_2S on membrane separation performance can be examined by analyzing the change in CO_2/CH_4 selectivity between the single component, binary and ternary cases. Figure 3 highlights these changes.

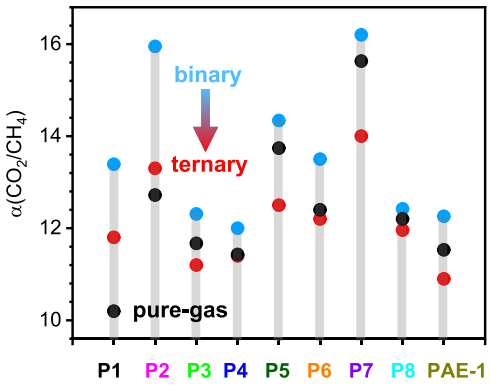

Figure 3. CO_2/CH_4 selectivity in binary (50:50 CO_2/CH_4 at 2.2 bar) and ternary (20:20:60 $H_2S/CO_2/CH_4$ at 8 bar) mixtures as well as corresponding calculated pure-gas selectivity ($f_{CH_4} = f_{CO_2}$ = 1.1 bar).

First, CO_2/CH_4 selectivity generally increases between the pure-gas calculations to the binary tests, demonstrating the role of competitive sorption when plasticization is minimal. Next, comparing the binary to the ternary tests, the reduction in selectivity becomes apparent across all samples. These findings are partially affected by the competition between H_2S and CO_2, whereby CO_2 is slightly excluded by H_2S and vice versa, and H_2S-induced plasticization likely reduces permselectivity in these polymers by diminishing size-sieving ability. Specifically, in the membranes where the combined acid-gas selectivity decreases most significantly when comparing pure- and mixed-gas performance (**P7** and **P8**), CH_4 permeability remains roughly unchanged between pure- and mixed-gas conditions. This finding suggests that H_2S-induced polymer dilation, while not enough to significantly increase CH_4 permeability, still likely occurs in these membranes to a larger degree than in the other materials, where CH_4 permeability decreases in all cases (see Tables S5 and S6 for all permeability data). Furthermore, tertiary amines do not contain hydrogen bond donors, and hence their structures are less stable than those with strong secondary forces. Additionally, the series of samples in this study do not contain cross-links, which are known to mitigate plasticization effects.[48−50] Harrigan et al. were able to show stable CO_2/CH_4 selectivity in both binary and ternary mixtures with cross-linked PEG membranes, and they attributed this stability to enhanced plasticization resistance afforded by reduced chain mobility.[51] Therefore, even highly flexible and low-T_g polymers, like the aforementioned PEG-based polymers, can be modified to induce stability to plasticization.[52] The polymers in this study, conversely, are still susceptible to plasticization despite their rigid structure. The high uptake of H_2S during operating conditions likely exacerbates plasticization effects in these samples, indicating that linear microporous polymers are still susceptible to these effects if not modified to add strong secondary forces or cross-links into the structures.

Although rarely reported in the open literature, the reduction in CO_2/CH_4 selectivity exhibited by our materials is consistent with trends reported for other glassy polymer membranes evaluated for separation of H_2S-based mixtures[53] and highlights the need for plasticization resistance against aggressive feed conditions. Of note, the partial fugacities of CO_2 and CH_4 in the binary case ($f_{CH_4} = f_{CO_2}$ = 1.1 bar) are slightly different than those in the ternary case (f_{CH_4} = 4.7 bar, f_{CO_2} = 1.5 bar). To investigate if partial pressure played a

https://doi.org/10.1021/jacsau.4c00489
JACS Au 2024, 4, 3848−3856

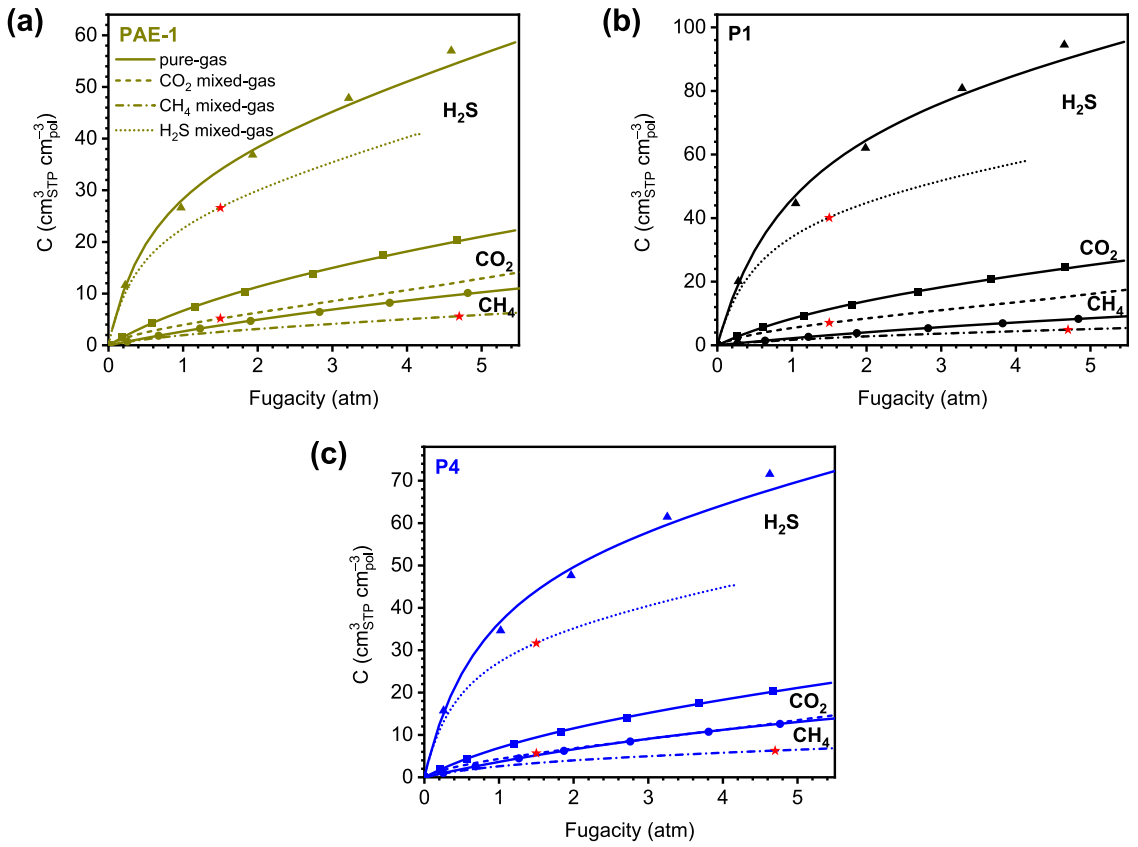

Figure 4. H_2S (triangles), CO_2 (squares), and CH_4 (circles) pure-gas sorption isotherms with DMS model fits (solid lines) and mixed-gas sorption predictions (dashed lines) for (a) **PAE-1**, (b) **P1**, and (c) **P4** in a 20:20:60 $H_2S/CO_2/CH_4$ mixture at 35 °C. Starred red data points are used for sorption selectivity predictions in Figure 5a. Note that sorption data obtained beyond 6 atm were used for determining model fits and predictions, and the full isotherms can be found in Figure S7.

significant role in our results, we performed binary experiments for CO_2/CH_4 mixtures with f_{CO_2} = 1.5 bar and f_{CH_4} = 4.7 bar for both **PAE-1** and **P5**. The selectivity of both **PAE-1** (13 ± 1) and **P5** (13 ± 1) were within experimental error of the selectivities found for these same materials in a 50/50 binary mixture at 2.2 total bar (13 ± 1 and 14 ± 1 for **PAE-1** and **P5**, respectively), suggesting that our comparisons are reasonable to support our proposed interpretation. Indeed, other researchers have reported that mixture selectivity in microporous polymers changes by less than 15% for more significant compositional and pressure sweeps of CO_2 and CH_4 mixtures.[27,41,54] For example, Swaidan et al. found that CO_2/CH_4 selectivity in AO-PIM-1 only decreased from 23 to 20 over an 8-bar CO_2 partial pressure sweep in a 50:50 mixture.[54] Hence, the comparison of selectivities in Figure 3 is appropriate given the limited dependence of binary selectivity on partial fugacity.

To connect materials separation performance in Figure 2 to transport theory, high-pressure sorption isotherms of H_2S, CO_2, and CH_4 at 35 °C were collected for **PAE-1**, **P1**, and **P4** in order to evaluate the role of competitive sorption on the resultant mixed-gas separation performance in both binary (CO_2/CH_4) and ternary ($H_2S/CO_2/CH_4$) mixtures. These specific materials were chosen in order to compare sorption results in cases where the permselectivity enhancement was largely absent (**P4**) and where it was present (**P1**). **PAE-1** was selected to serve as the control material. Sorption in glassy polymers is often described by the dual-mode sorption (DMS) model[55,56]

$$C_{i,\text{pure}} = k_{D,i} f_i + \frac{C'_{H,i} b_i f_i}{1 + b_i f_i} \quad (1)$$

where C_i is the concentration of gas i in the polymer (cm_{STP}^3 cm_{pol}^{-3}), $k_{D,i}$ is the Henry's law constant (cm_{STP}^3 cm_{pol}^{-3} atm^{-1}), $C'_{H,i}$ is the Langmuir sorption capacity (cm_{STP}^3 cm_{pol}^{-3}), b_i is the Langmuir affinity constant (atm^{-1}), and f_i is the equilibrium fugacity (atm). Although the first term of eq 1 represents the population of gases dissolved in the hypothetical Henry's mode of the polymer, the second term in the equation describes the population of gases sorbed in the nonequilibrium Langmuir mode. With regard to this study, all pure-gas sorption isotherms were fitted using a high-precision MATLAB optimization method developed by Wu et al.,[57] as was done in our previous work.[58] With the fitted DMS parameters, which are shown in Tables S7−S9, we then used an extension of the DMS model to predict mixed-gas sorption isotherms, which are exceedingly difficult to measure experimentally.[59,60] This extension is shown below[61]

$$C_{i,\text{mixed}} = k_{D,i} f_i + \frac{C'_{H,i} b_i f_i}{1 + b_i f_i + b_j f_j + b_k f_k} \quad (2)$$

where i is the component of interest and j and k are other gases in the mixture. The resultant fitted pure-gas isotherms and predicted mixed-gas sorption isotherms for a ternary (20:20:60 $H_2S/CO_2/CH_4$ at 8 bar) mixture can be found in Figure 4.

As can be gleaned from Figure 4, the uptake of all three gases predictably drops in the presence of a mixture due to the

https://doi.org/10.1021/jacsau.4c00489
JACS Au 2024, 4, 3848−3856

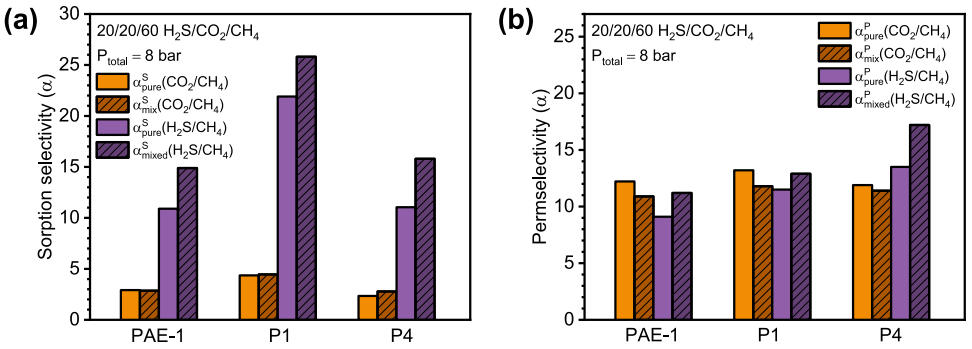

Figure 5. (a) Pure-gas CO_2/CH_4 (orange bars) and H_2S/CH_4 (purple bars) sorption selectivities ($\alpha^S_{i/j}$) and modeled mixed-gas CO_2/CH_4 (dark brown and patterned bars) and H_2S/CH_4 (dark purple and patterned bars) sorption selectivities for **PAE-1**, **P1**, and **P4** in a 20:20:60 $H_2S/CO_2/CH_4$ mixture. (b) Pure-gas CO_2/CH_4 (orange bars) and H_2S/CH_4 (purple bars) permselectivities ($\alpha^P_{i/j}$) and measured mixed-gas CO_2/CH_4 (dark brown and patterned bars) and H_2S/CH_4 (dark purple and patterned bars) permselectivities for **PAE-1**, **P1**, and **P4** in a 20:20:60 $H_2S/CO_2/CH_4$ mixture.

exclusion of competing species in the sorbed phase. Thus, modeling within the framework of the dual-mode model enables a comparison for how the sorption selectivity changes between the pure- and mixed-gas scenarios. Extending this analysis to the sorption−diffusion model, permselectivity ($\alpha^P_{i/j}$) can be represented as the product of diffusion selectivity ($\alpha^D_{i/j}$) and sorption selectivity ($\alpha^S_{i/j}$):

$$\alpha_{i/j} = \frac{P_i}{P_j} = \frac{D_i S_i}{D_j S_j} = \left(\frac{D_i}{D_j}\right) = \left(\frac{S_i}{S_j}\right) = \alpha^D_{i/j} \times \alpha^S_{i/j} \quad (3)$$

Using the predicted sorption selectivity enhancement determined with eq 2, we can calculate the extent to which sorption selectivity drives the permselectivity increase that occurs when testing in a mixture, assuming the diffusion selectivity remains constant. A summary of both pure- and mixed-gas sorption selectivities and permselectivities are presented in Figure 5.

For CO_2/CH_4 separation in the ternary mixture, the sorption selectivities remain relatively constant, with the permselectivities seeing a slight decrease. This decrease can be interpreted as a result of the competition between H_2S and CO_2 as well as the plasticization induced by the presence of H_2S, which likely reduces CO_2/CH_4 diffusion selectivity and thus overall permselectivity. These slight decreases in permselectivity, in addition to the relatively constant sorption selectivities, are very similar to those exhibited by the nitrile-functional PIM-1 and PAE-CN from our previous study,[47] suggesting that the tertiary amine might interact with CO_2 in a similar manner than does the nitrile. Future energetics analysis using variable-temperature sorption isotherms are necessary to substantiate this claim.

Regarding H_2S/CH_4 separation, the relative increases in sorption selectivity appear to align more closely with the measured permselectivity increases, suggesting that this separation is driven by sorption effects, as has been noted in the literature for glassy polymers,[62] such as chemically modified polynorbornenes and polyimides.[53] However, when comparing the tertiary-amine-functional **P1** and **P4** to the unfunctionalized **PAE-1**, it appears that the enhanced H_2S affinity shown in the sorption isotherms in Figures 4 and S7, which can be attributed to the amine group, does not fully translate to enhanced H_2S-based mixed-gas separation performance. The mixed-gas H_2S/CH_4 permselectivity of **P4** is only 54% higher than that of **PAE-1**, and the permselectivity of **P1** is only 15% higher. Both of these results are accompanied by decreases in acid-gas permeability. Additionally, the predicted pure- to mixed-gas increases in H_2S/CH_4 sorption selectivity for each selected polymer (37% for **PAE-1**, 18% for **P1**, and 43% for **P4**, respectively) are all slightly higher than the measured permselectivity increases (23, 12, and 27%, respectively). As previously mentioned, it is worth noting that competition between H_2S and co-permeating CO_2 also contributes to a reduced H_2S/CH_4 selectivity given the weak ability of CO_2 to exclude some H_2S. However, given that the fitted Langmuir affinity parameter for H_2S is substantially higher than that for CO_2 in each polymer, it seems that a diminished H_2S/CH_4 diffusion selectivity brought on by the aforementioned plasticizing behavior of H_2S is likely a larger driver in reducing the overall permselectivity.

Interestingly, the high value of the predicted H_2S/CH_4 sorption selectivity for **P1** in Figure 5a implies that the corresponding H_2S/CH_4 diffusion selectivity in the mixed-gas experiment is less than 1. This result is unexpected since H_2S has a smaller kinetic diameter than CH_4. There are a few possible reasons for this finding. First, we acknowledge the ongoing debate in the literature about the quality of fitting mixed-gas sorption behavior from DMS parameters, which admittedly decreases our confidence in drawing mechanistic conclusions from these small differences.[59] Second, we note the role of hindered diffusion for strongly sorbing functional groups in microporous polymers. It is well-known that the transport diffusivity of CO_2 in PIM-NH_2 is reduced due to the strong sorption of CO_2 in the polymer.[27,47,63] Although tertiary amines have weaker interactions, it is possible that the small but inverted diffusion selectivity we are reporting here is a result of H_2S having more strongly hindered diffusion than CH_4 in these mixtures. Indeed, more significant trends for inverted diffusion selectivity have been observed for PIM-NH_2 and PAE-NH_2 for H_2S/CH_4 separations.[47,58] The inversion in diffusion selectivity does not occur for **P4** (1.1 diffusion selectivity), and while this inversion does indeed occur in **PAE-1**, it is not as significant as in **P1** (0.75 vs 0.5 diffusion selectivity, respectively). Notably, both **PAE-1** and **P4** have lower H_2S sorption than **P1** (cf., Figure S7) despite **PAE-1** exhibiting higher FFV and BET surface area. Thus, it is possible that diffusion selectivity in these strongly sorbing mixtures inverts at a certain threshold of sorption energetics. This potential co-dependency between sorption and diffusion provides a fascinating topic of future study within the

https://doi.org/10.1021/jacsau.4c00489
JACS Au 2024, 4, 3848−3856

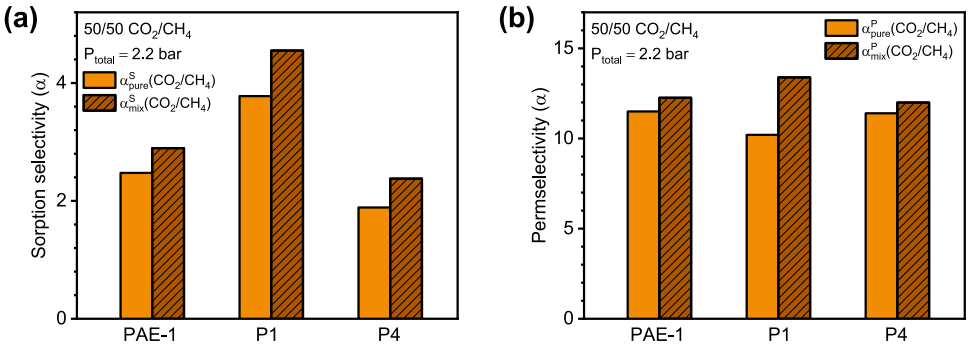

Figure 6. (a) Pure-gas CO_2/CH_4 (orange bars) sorption selectivities ($\alpha^S_{CO_2/CH_4}$) and modeled mixed-gas CO_2/CH_4 (dark brown and patterned bars) sorption selectivities for **PAE-1**, **P1**, and $\mathbf{P_4}$ in a 50:50 CO_2/CH_4 mixture. (b) Pure-gas CO_2/CH_4 (orange bars) permselectivities ($\alpha^P_{CO_2/CH_4}$) and measured mixed-gas CO_2/CH_4 (dark brown and patterned bars) permselectivities for **PAE-1**, **P1**, and **P4** in a 50:50 CO_2/CH_4 mixture.

sorption−diffusion model. For gas separations, correcting transport diffusivities to thermodynamically corrected diffusivities is rare, and there are opportunities to leverage insights from the Darken Equation and the Maxwell−Stefan framework to better understand the fundamentals of complex mixture separations for microporous polymers that contain functional groups that have strong affinity to gas species.[64,65]

For the binary (50:50 CO_2/CH_4) tests at 2.2 bar, we performed the same mixed-gas prediction analyses as above. These results are summarized in Figure 6. For this comparison, we can see that there is a correlation between the predicted sorption selectivity enhancement and the measured boost in permselectivity, especially when compared to the opposite trend that was shown for CO_2/CH_4 selectivity in the ternary mixtures of Figure 5. For example, the predicted sorption selectivity increase in **P1** is 20%, while the observed permselectivity increase in the binary mixture is 31%. As opposed to the ternary tests, which were conducted at 8 bar total pressure with H_2S included in the mixture, the binary experiments were performed at 2.2 bar, which should make plasticization effects much less observable. CO_2 also sorbs less strongly than H_2S in these polymers. As a result, the sorption enhancements are preserved in the mixed-gas permeation experiments, leading to permselectivity increases that mirror those of the sorption selectivity.

In conclusion, we have synthesized eight tertiary-amine-functional porous PAEs for acid-gas separations and investigated the effects of competitive sorption on their mixed-gas separation performance in binary (CO_2/CH_4) and ternary ($H_2S/CO_2/CH_4$) mixtures. Through chloromethylation and nucleophilic substitution, a variety of amine side groups can be easily installed, producing polymers that are fully solution-processable and have good physical stability. Through DMS modeling and mixed-gas sorption predictions, we observed that the effects of competitive sorption are beneficial for both the binary and ternary mixtures. However, improvements in permselectivity are more easily realized in the binary case than in the ternary case, which we attribute to the confounding impact of H_2S-induced plasticization in the ternary mixtures with high H_2S concentration, which can lower diffusion selectivity. Nevertheless, beneficial improvements from competitive sorption can offset negative declines in diffusion selectivity from plasticization in the ternary mixture case. Our synthetic approach provides a generalizable strategy to incorporate processable tertiary amines into microporous polymer membranes for the removal of acidic gases, and we further demonstrated how sorption analyses and mixed-gas sorption predictions can be used to better understand the role of chemical functionality in the separation performance of this unique subclass of PAEs.

■ ASSOCIATED CONTENT

Supporting Information

The Supporting Information is available free of charge at https://pubs.acs.org/doi/10.1021/jacsau.4c00489.

Detailed synthesis and characterization data; also available are sorption isotherms, dual-mode fitting analyses, and complete permeability data (PDF)

■ AUTHOR INFORMATION

Corresponding Authors

Timothy M. Swager − *Department of Chemistry, Massachusetts Institute of Technology, Cambridge, Massachusetts 02139, United States;* orcid.org/0000-0002-3577-0510; Email: tswager@mit.edu

Zachary P. Smith − *Department of Chemical Engineering, Massachusetts Institute of Technology, Cambridge, Massachusetts 02139, United States;* orcid.org/0000-0002-9630-5890; Email: zpsmith@mit.edu

Authors

Pablo A. Dean − *Department of Chemical Engineering, Massachusetts Institute of Technology, Cambridge, Massachusetts 02139, United States*

Yifan Wu − *Department of Chemistry, Massachusetts Institute of Technology, Cambridge, Massachusetts 02139, United States;* orcid.org/0000-0002-8949-1250

Sheng Guo − *Department of Chemistry, Massachusetts Institute of Technology, Cambridge, Massachusetts 02139, United States*

Complete contact information is available at: https://pubs.acs.org/10.1021/jacsau.4c00489

Author Contributions

§P.A.D. and Y.W. contributed equally to this work and are co-first authors.

Notes

The authors declare no competing financial interest.

https://doi.org/10.1021/jacsau.4c00489
JACS Au 2024, 4, 3848−3856

■ ACKNOWLEDGMENTS

This work was supported by the Department of Navy, Office of Naval Research under ONR awards N00014-20-1-2418 and N00014-21-1-2666 for support in the development and testing of novel microporous polymers and for support in elucidating the role of competitive sorption in membrane materials. Additionally, we are grateful to Eni S.p.A. through the MIT Energy Initiative for support in polymer development for H_2S-based separations. P.A.D. acknowledges support from an NSF-GRFP fellowship (DGE-2141064). T.M.S. is grateful for support from the National Science Foundation DMR-2207299. This study made use of the shared facilities available at MIT, including the Materials Research Laboratory and the Department of Chemistry Instrumentation Facility.

■ REFERENCES

(1) Sholl, D. S.; Lively, R. P. Seven Chemical Separations to Change the World. *Nature* **2016**, *532* (7600), 435−437.
(2) Valappil, R. S. K.; Ghasem, N.; Al-Marzouqi, M. Current and Future Trends in Polymer Membrane-Based Gas Separation Technology: A Comprehensive Review. *J. Ind. Eng. Chem.* **2021**, *98*, 103−129.
(3) Galizia, M.; Chi, W. S.; Smith, Z. P.; Merkel, T. C.; Baker, R. W.; Freeman, B. D. 50th Anniversary Perspective: Polymers and Mixed Matrix Membranes for Gas and Vapor Separation: A Review and Prospective Opportunities. *Macromolecules* **2017**, *50* (20), 7809−7843.
(4) Sanders, D. F.; Smith, Z. P.; Guo, R.; Robeson, L. M.; McGrath, J. E.; Paul, D. R.; Freeman, B. D. Energy-Efficient Polymeric Gas Separation Membranes for a Sustainable Future: A Review. *Polymer* **2013**, *54* (18), 4729−4761.
(5) Bernardo, P.; Drioli, E.; Golemme, G. Membrane Gas Separation: A Review/State of the Art. *Ind. Eng. Chem. Res.* **2009**, *48* (10), 4638−4663.
(6) Hassan, T. N. A. T.; Shariff, A. M.; Pauzi, M. M. M.; Khidzir, M. S.; Surmi, A. Insights on Cryogenic Distillation Technology for Simultaneous CO_2 and H_2S Removal for Sour Gas Fields. *Molecules* **2022**, *27* (4), No. 1424.
(7) Merkel, T. C.; Lin, H.; Wei, X.; Baker, R. Power Plant Post-Combustion Carbon Dioxide Capture: An Opportunity for Membranes. *J. Membr. Sci.* **2010**, *359* (1−2), 126−139.
(8) Baker, R. W.; Lokhandwala, K. Natural Gas Processing with Membranes: An Overview. *Ind. Eng. Chem. Res.* **2008**, *47* (7), 2109−2121.
(9) Alcheikhhamdon, Y.; Hoorfar, M. Natural Gas Purification from Acid Gases Using Membranes: A Review of the History, Features, Techno-Commercial Challenges, and Process Intensification of Commercial Membranes. *Chem. Eng. Process.* **2017**, *120*, 105−113.
(10) Assunção, L. R. C.; Mendes, P. A. S.; Matos, S.; Borschiver, S. Technology Roadmap of Renewable Natural Gas: Identifying Trends for Research and Development to Improve Biogas Upgrading Technology Management. *Appl. Energy* **2021**, *292*, No. 116849.
(11) Yu, C. H.; Huang, C. H.; Tan, C. S. A Review of CO_2 Capture by Absorption and Adsorption. *Aerosol Air Qual. Res.* **2012**, *12* (5), 745−769.
(12) Babamohammadi, S.; Shamiri, A.; Aroua, M. K. A Review of CO_2 Capture by Absorption in Ionic Liquid-Based Solvents. *Rev. Chem. Eng.* **2015**, *31* (4), 383−412.
(13) Farnam, M.; Mukhtar, H.; Shariff, A. M. A Review on Glassy Polymeric Membranes for Gas Separation. *Appl. Mech. Mater.* **2014**, *625*, 701−703.
(14) Robeson, L. M. The Upper Bound Revisited. *J. Membr. Sci.* **2008**, *320* (1−2), 390−400.
(15) Bandehali, S.; Ebadi Amooghin, A.; Sanaeepur, H.; Ahmadi, R.; Fuoco, A.; Jansen, J. C.; Shirazian, S. Polymers of Intrinsic Microporosity and Thermally Rearranged Polymer Membranes for Highly Efficient Gas Separation. *Sep. Purif. Technol.* **2021**, *278*, No. 119513.
(16) Long, T. M.; Swager, T. M. Molecular Design of Free Volume as a Route to Low-κ Dielectric Materials. *J. Am. Chem. Soc.* **2003**, *125* (46), 14113−14119.
(17) Budd, P. M.; Ghanem, B. S.; Makhseed, S.; McKeown, N. B.; Msayib, K. J.; Tattershall, C. E. Polymers of Intrinsic Microporosity (PIMs): Robust, Solution-Processable, Organic Nanoporous Materials. *Chem. Commun.* **2004**, *4* (2), 230−231.
(18) Budd, P. M.; Msayib, K. J.; Tattershall, C. E.; Ghanem, B. S.; Reynolds, K. J.; McKeown, N. B.; Fritsch, D. Gas Separation Membranes from Polymers of Intrinsic Microporosity. *J. Membr. Sci.* **2005**, *251* (1−2), 263−269.
(19) Carta, M.; Malpass-Evans, R.; Croad, M.; Rogan, Y.; Jansen, J. C.; Bernardo, P.; Bazzarelli, F.; McKeown, N. B. An Efficient Polymer Molecular Sieve for Membrane Gas Separations. *Science* **2013**, *339* (6117), 303−307.
(20) Lai, H. W. H.; Benedetti, F. M.; Ahn, J. M.; Robinson, A. M.; Wang, Y.; Pinnau, I.; Smith, Z. P.; Xia, Y. Hydrocarbon Ladder Polymers with Ultrahigh Permselectivity for Membrane Gas Separations. *Science* **2022**, *375* (6587), 1390−1392.
(21) Baker, R. W.; Low, B. T. Gas Separation Membrane Materials: A Perspective. *Macromolecules* **2014**, *47* (20), 6999−7013.
(22) Sanders, E. S.; Jordan, S. M.; Subramanian, R. Penetrant-Plasticized Permeation in Polymethylmethacrylate. *J. Membr. Sci.* **1992**, *74* (1−2), 29−39.
(23) Wessling, M.; Schoeman, S.; van der Boomgaard, T.; Smolders, C. A. Plasticization of Gas Separation Membranes. *Gas Sep. Purif.* **1991**, *5* (4), 222−228.
(24) Vopička, O.; De Angelis, M. G.; Sarti, G. C. Mixed Gas Sorption in Glassy Polymeric Membranes: I. CO_2/CH_4 and n-C_4/CH_4 Mixtures Sorption in Poly(1-Trimethylsilyl-1-Propyne) (PTMSP). *J. Membr. Sci.* **2014**, *449*, 97−108.
(25) Vopička, O.; De Angelis, M. G.; Du, N.; Li, N.; Guiver, M. D.; Sarti, G. C. Mixed Gas Sorption in Glassy Polymeric Membranes: II. CO_2/CH_4 Mixtures in a Polymer of Intrinsic Microporosity (PIM-1). *J. Membr. Sci.* **2014**, *459*, 264−276.
(26) Rodriguez, K. M.; Lin, S.; Wu, A. X.; Han, G.; Teesdale, J. J.; Doherty, C. M.; Smith, Z. P. Leveraging Free Volume Manipulation to Improve the Membrane Separation Performance of Amine-Functionalized PIM-1. *Angew. Chem.* **2021**, *133* (12), 6667−6673.
(27) Rodriguez, K. M.; Benedetti, F. M.; Roy, N.; Wu, A. X.; Smith, Z. P. Sorption-Enhanced Mixed-Gas Transport in Amine Functionalized Polymers of Intrinsic Microporosity (PIMs). *J. Mater. Chem. A* **2021**, *9* (41), 23631−23642.
(28) Lepaumier, H.; Picq, D.; Carrette, P. L. New Amines for CO_2 Capture. II. Oxidative Degradation Mechanisms. *Ind. Eng. Chem. Res.* **2009**, *48* (20), 9068−9075.
(29) Guo, S.; Swager, T. M. Versatile Porous Poly(Arylene Ether)s via Pd-Catalyzed C-O Polycondensation. *J. Am. Chem. Soc.* **2021**, *143* (30), 11828−11835.
(30) Lee, M.; Bezzu, C. G.; Carta, M.; Bernardo, P.; Clarizia, G.; Jansen, J. C.; McKeown, N. B. Enhancing the Gas Permeability of Tröger's Base Derived Polyimides of Intrinsic Microporosity. *Macromolecules* **2016**, *49* (11), 4147−4154.
(31) Dong, G.; Lee, Y. M. Microporous Polymeric Membranes Inspired by Adsorbent for Gas Separation. *J. Mater. Chem. A* **2017**, *5*, 13294−13319.
(32) Ma, X.; Pinnau, I. A Novel Intrinsically Microporous Ladder Polymer and Copolymers Derived from 1,1′,2,2′-Tetrahydroxy-Tetraphenylethylene for Membrane-Based Gas Separation. *Polym. Chem.* **2016**, *7* (6), 1244−1248.
(33) Guo, S.; Yeo, J. Y.; Benedetti, F. M.; Syar, D.; Swager, T. M.; Smith, Z. P. A Microporous Poly(Arylene Ether) Platform for Membrane-Based Gas Separation. *Angew. Chem., Int. Ed.* **2024**, *63* (8), No. e202315611.
(34) Rouquerol, J.; Llewellyn, P.; Rouquerol, F. Is the BET Equation Applicable to Microporous Adsorbents? *Stud. Surf. Sci. Catal.* **2007**, *160*, 49−56.

https://doi.org/10.1021/jacsau.4c00489
JACS Au 2024, 4, 3848−3856

(35) Wu, A. X.; Lin, S.; Rodriguez, K. M.; Benedetti, F. M.; Joo, T.; Grosz, A. F.; Storme, K. R.; Roy, N.; Syar, D.; Smith, Z. P. Revisiting Group Contribution Theory for Estimating Fractional Free Volume of Microporous Polymer Membranes. *J. Membr. Sci.* **2021**, *636*, No. 119526.
(36) Weber, J.; Meng, Q. B. Microporous Polymers: Synthesis, Characterization, and Applications. In *Encyclopedia of Polymer Science and Technology*; John Wiley & Sons, Inc, 2002.
(37) Hart, K. E.; Abbott, L. J.; Colina, C. M. Analysis of Force Fields and BET Theory for Polymers of Intrinsic Microporosity. *Mol. Simul.* **2013**, *39* (5), 397−404.
(38) Yin, H.; Chua, Y. Z.; Yang, B.; Schick, C.; Harrison, W. J.; Budd, P. M.; Böhning, M.; Schönhals, A. First Clear-Cut Experimental Evidence of a Glass Transition in a Polymer with Intrinsic Microporosity: PIM-1. *J. Phys. Chem. Lett.* **2018**, *9* (8), 2003−2008.
(39) McKeown, N. B.; Budd, P. M. Polymers of Intrinsic Microporosity (PIMs): Organic Materials for Membrane Separations, Heterogeneous Catalysis and Hydrogen Storage. *Chem. Soc. Rev.* **2006**, *35* (8), 675−683.
(40) Zhuang, Y.; Seong, J. G.; Do, Y. S.; Jo, H. J.; Cui, Z.; Lee, J.; Lee, Y. M.; Guiver, M. D. Intrinsically Microporous Soluble Polyimides Incorporating Trögers Base for Membrane Gas Separation. *Macromolecules* **2014**, *47* (10), 3254−3262.
(41) Park, H. B.; Jung, C. H.; Lee, Y. M.; Hill, A. J.; Pas, S. J.; Mudie, S. T.; Van Wagner, E.; Freeman, B. D.; Cookson, D. J. Polymers with Cavities Tuned for Fast Selective Transport of Small Molecules and Ions. *Science* **2007**, *318* (5848), 254−258.
(42) He, Y.; Benedetti, F. M.; Lin, S.; Liu, C.; Zhao, Y.; Ye, H. Z.; van Voorhis, T.; de Angelis, M. G.; Swager, T. M.; Smith, Z. P. Polymers with Side Chain Porosity for Ultrapermeable and Plasticization Resistant Materials for Gas Separations. *Adv. Mater.* **2019**, *31* (21), No. 1807871.
(43) Wang, Y.; Ma, X.; Ghanem, B. S.; Alghunaimi, F.; Pinnau, I.; Han, Y. Polymers of Intrinsic Microporosity for Energy-Intensive Membrane-Based Gas Separations. *Mater. Today Nano* **2018**, *3* (2018), 69−95.
(44) Liu, G.; Chernikova, V.; Liu, Y.; Zhang, K.; Belmabkhout, Y.; Shekhah, O.; Zhang, C.; Yi, S.; Eddaoudi, M.; Koros, W. J. Mixed Matrix Formulations with MOF Molecular Sieving for Key Energy-Intensive Separations. *Nat. Mater.* **2018**, *17* (3), 283−289.
(45) Comesaña-Gándara, B.; Chen, J.; Bezzu, C. G.; Carta, M.; Rose, I.; Ferrari, M. C.; Esposito, E.; Fuoco, A.; Jansen, J. C.; McKeown, N. B. Redefining the Robeson Upper Bounds for CO_2/CH_4 and CO_2/N_2 Separations Using a Series of Ultrapermeable Benzotriptycene-Based Polymers of Intrinsic Microporosity. *Energy Environ. Sci.* **2019**, *12* (9), 2733−2740.
(46) Robeson, L. M. Correlation of Separation Factor versus Permeability for Polymeric Membranes. *J. Membr. Sci.* **1991**, *62* (2), 165−185.
(47) Rodriguez, K. M.; Dean, P. A.; Guo, S.; Roy, N.; Swager, T. M.; Smith, Z. P. Elucidating the Role of Micropore-Generating Backbone Motifs and Amine Functionality on Membrane Separation Performance in Complex Mixtures. *J. Membr. Sci.* **2024**, *696*, No. 122464.
(48) Qiu, W.; Chen, C. C.; Xu, L.; Cui, L.; Paul, D. R.; Koros, W. J. Sub-T_g Cross-Linking of a Polyimide Membrane for Enhanced CO_2 Plasticization Resistance for Natural Gas Separation. *Macromolecules* **2011**, *44* (15), 6046−6056.
(49) Kim, J. H.; Koros, W. J.; Paul, D. R. Effects of CO_2 Exposure and Physical Aging on the Gas Permeability of Thin 6FDA-Based Polyimide Membranes. Part 2. with Crosslinking. *J. Membr. Sci.* **2006**, *282* (1−2), 32−43.
(50) Staudt-Bickel, C.; Koros, W. J. Improvement of CO_2/CH_4 Separation Characteristics of Polyimides by Chemical Crosslinking. *J. Membr. Sci.* **1999**, *155* (1), 145−154.
(51) Harrigan, D. J.; Lawrence, J. A.; Reid, H. W.; Rivers, J. B.; O'Brien, J. T.; Sharber, S. A.; Sundell, B. J. Tunable Sour Gas Separations: Simultaneous H_2S and CO_2 Removal from Natural Gas via Crosslinked Telechelic Poly(Ethylene Glycol) Membranes. *J. Membr. Sci.* **2020**, *602*, No. 117947.
(52) Hayek, A.; Yahaya, G. O.; Alsamah, A.; Alghannam, A. A.; Jutaily, S. A.; Mokhtari, I. Pure - and Sour Mixed-Gas Transport Properties of 4,4′-Methylenebis(2,6-Diethylaniline)-Based Copolyimide Membranes. *Polymer* **2019**, *166*, 184−195.
(53) Liu, Y.; Liu, Z.; Liu, G.; Qiu, W.; Bhuwania, N.; Chinn, D.; Koros, W. J. Surprising Plasticization Benefits in Natural Gas Upgrading Using Polyimide Membranes. *J. Membr. Sci.* **2020**, *593*, No. 117430.
(54) Swaidan, R.; Ghanem, B. S.; Litwiller, E.; Pinnau, I. Pure- and Mixed-Gas CO_2/CH_4 Separation Properties of PIM-1 and an Amidoxime-Functionalized PIM-1. *J. Membr. Sci.* **2014**, *457*, 95−102.
(55) Paul, D. R. Effect of Immobilizing Adsorption on the Diffusion Time Lag. *J. Polym. Sci., Part A-2* **1969**, *7* (10), 1811−1818.
(56) Fredrickson, G. H.; Helfand, E. Dual-Mode Transport of Penetrants in Glassy Polymers. *Macromolecules* **1985**, *18* (11), 2201−2207.
(57) Wu, A. X.; Drayton, J. A.; Rodriguez, K. M.; Benedetti, F. M.; Qian, Q.; Lin, S.; Smith, Z. P. Elucidating the Role of Fluorine Content on Gas Sorption Properties of Fluorinated Polyimides. *Macromolecules* **2021**, *54* (1), 22−34.
(58) Dean, P. A.; Rodriguez, K. M.; Guo, S.; Roy, N.; Swager, T. M.; Smith, Z. P. Elucidating the Role of Micropore-Generating Backbone Motifs and Amine Functionality on H_2S, CO_2, CH_4 and N_2 Sorption. *J. Membr. Sci.* **2024**, *696*, No. 122465.
(59) Ricci, E.; De Angelis, M. G. Modelling Mixed-Gas Sorption in Glassy Polymers for CO_2 Removal: A Sensitivity Analysis of the Dual Mode Sorption Model. *Membranes* **2019**, *9* (1), No. 8.
(60) Ricci, E.; Benedetti, F. M.; Dose, M. E.; De Angelis, M. G.; Freeman, B. D.; Paul, D. R. Competitive Sorption in CO_2/CH_4 Separations: The Case of HAB-6FDA Polyimide and Its TR Derivative and a General Analysis of Its Impact on the Selectivity of Glassy Polymers at Multicomponent Conditions. *J. Membr. Sci.* **2020**, *612*, No. 118374.
(61) Koros, W. J. Model for sorption of mixed gases in glassy polymers. *J. Polym. Sci., Polym. Phys. Ed.* **1980**, *18* (5), 981−992.
(62) Deng, J.; Huang, Z.; Sundell, B. J.; Harrigan, D. J.; Sharber, S. A.; Zhang, K.; Guo, R.; Galizia, M. State of the Art and Prospects of Chemically and Thermally Aggressive Membrane Gas Separations: Insights from Polymer Science. *Polymer* **2021**, *229*, No. 123988.
(63) Mason, C. R.; Maynard-Atem, L.; Heard, K. W. J.; Satilmis, B.; Budd, P. M.; Friess, K.; Lancì, M.; Bernardo, P.; Clarizia, G.; Jansen, J. C. Enhancement of CO_2 Affinity in a Polymer of Intrinsic Microporosity by Amine Modification. *Macromolecules* **2014**, *47* (3), 1021−1029.
(64) Darken, L. S. Diffusion, Mobility and Their Interrelation through Free Energy in Binary Metallic Systems. *Trans. AIME* **1948**, *175*, 184−201.
(65) Stewart, W. E. Multicomponent Mass Transfer. By Ross Taylor and R. Krishna, Wiley, New York, 1993, 579 Pp. *AIChE J.* **1995**, *41* (1), 202−203.

https://doi.org/10.1021/jacsau.4c00489
JACS Au 2024, 4, 3848−3856